

Modeling of Machining Force in Hard Turning Process

Souâd MAKHFI*, Kamel HADDOUCHE**, Abdelghafour BOURDIM***, Malek HABAK****

*Laboratory of Industrial Technologies, Ibn Khaldun University of Tiaret, B. P. 78 Tiaret 14000, Algeria, E-mail: msouad71@gmail.com

**Laboratory of Industrial Technologies, Ibn Khaldun University of Tiaret, B. P. 78 Tiaret 14000, Algeria, E-mail: haddouchekam@gmail.com

***Laboratory of Water and Constructions in their Environment, Abou Bekr Belkeid University of Tlemcen, B. P. 230 Chetouane 13000 Tlemcen, Algeria, E-mail: bourdim56@yahoo.fr

****Laboratory of Innovate Technologies, Picardie Jules Verne University of Amiens, Avenue des Facultés, Le Bailly 80025 Amiens Cedex 1, France, E-mail: malek.habak@u-picardie.fr

crossref <http://dx.doi.org/10.5755/j01.mech.24.3.19146>

1. Introduction

In machining process, cutting forces are factors that manufacturers must control to ensure better performances. Cutting forces are reliable variables; for this purpose, they were used in various applications such as the adaptive control, the monitoring and the on-line estimation of tool wear. Modeling of machining forces is one of the major problems in the theory of cutting. Many parameters influence greatly the machining forces, so it is quite difficult to develop a theoretical model to describe efficiently the cutting process. The problem of modeling or predicting machining forces has been investigated by many researchers [1-12].

In this study, an ANN approach is proposed to predict machining force components in hard turning of an AISI 52100 bearing steel using CBN cutting tool. Machining parameters such as cutting speed, feed, dept-of-cut and workpiece hardness are taken as inputs of the ANN while machining force components such as feed-force, radial-force and tangential-force are the outputs. To show the effectiveness of the developed ANN, the results of machining force prediction will be confronted with experimental data. Also, the ANN results were compared to those obtained by MLR model.

2. ANN approach and MLR modeling

The neural network approach is a technique based on the statistical regression. It can be used in various fields of engineering for modeling complex relationships which are difficult to describe by physical models.

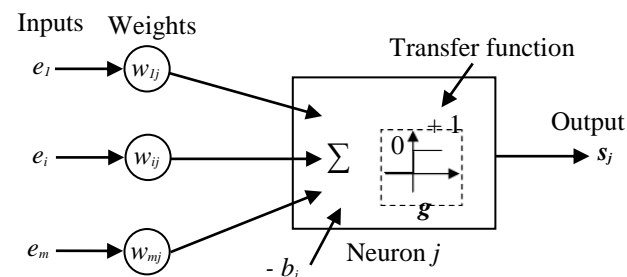


Fig. 1 Mathematical model of an artificial neuron

An ANN consists of simple processors called neurons interconnected. The model of an artificial neuron is illustrated in Fig. 1 (model of McCulloch and Pitts [13]).

The neuron output s_j is calculated as:

$$s_j = g \left(\sum_{i=1}^m w_{ij} \cdot e_i - b_j \right). \quad (1)$$

When the activation level reaches or exceeds the bias b_j , then the argument of the transfer or activation function g , applied to the sum of the inputs, becomes positive (equal to +1); if not, it is zero. The bias is much like a weight, except that it has a constant input of -1.

Notice that weights w_{ij} of neuron inputs e_i and b_j are both adjustable scalar parameters of the neuron. Typically the transfer function is chosen by the designer and then the parameters w_{ij} and b_j will be adjusted by some learning or training algorithm so that the neuron input-output relationship meets some specific goal.

The ANN architecture has an input vector receiving input data, an output layer which sends final information to users, and in middle stand hidden layers which have no direct contact with the environment.

The developed ANN consists of multilayer feed-forward: input, hidden and output layers as illustrated in Fig. 2.

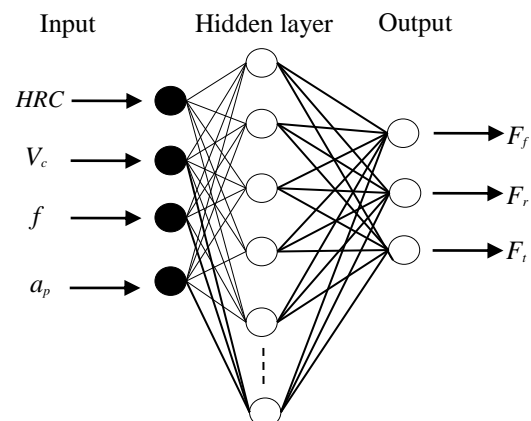


Fig. 2 Architecture of the developed ANN

Let us recall that the machining parameters such as cutting speed V_c , feed f , dept-of-cut a_p and workpiece hardness HRC are taken as input vector of the ANN while machining force components such as feed-force F_f , radial-force F_r and tangential-force F_t are the outputs.

Fig. 3 shows the cutting parameters and the cutting force components in turning process.

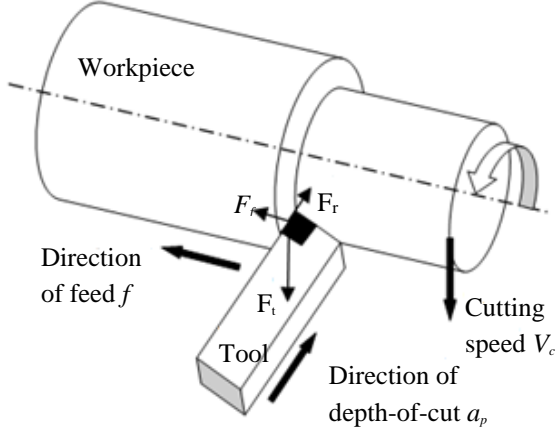


Fig. 3 Machining force components in turning process

The selection of transfer functions in the hidden and output layers, number of hidden layers and neurons in a hidden layer are very important to obtain the best prediction results. In this study, the optimal network architecture is determined after several simulations by Matlab Neural Network Toolbox. The methodology used to obtain the optimal network architecture is summarized below in section 2.2.

The basic goal in training is to minimize the overall error of the network between target or experimental data and network output, and then the best network structure was determined. The training is stopped when the validation error reaches a minimum value. For the developed ANN, Back-Propagation (BP) by Bayesian Regularization (BR) in combination with Levenberg–Marquardt (LM) algorithm is employed for training. Since, it has proved that BP algorithm is an excellent universal approximator of non-linear functions.

The performance evaluation of the optimum network architecture is determined by overall calculated statistical error values as SSE (Sum Squared Errors) and SSW (Sum Squared Weights) under Matlab Neural Network Toolbox for the ANN between target data and network output during training and testing phases. Additionally, to find the optimal network architecture, linear regression coefficient R Eq. (2) [14] and Mean Absolute Percentage Error MAPE Eq. (3) [10] between ANN prediction and experimental values are used to evaluate the statistical performance of the network for training and testing phases.

$$R = \frac{\sqrt{\sum_{k=1}^Q (s(k) - \bar{c})^2}}{\sqrt{\sum_{k=1}^Q (c(k) - s(k))^2 + \sum_{k=1}^Q (s(k) - \bar{c})^2}}. \quad (2)$$

$$MAPE(\%) = \frac{|c(k) - s(k)|}{c(k)}. \quad (3)$$

A linear regression model that contains more than one predictor variable is called a Multiple Linear Regression model. MLR attempts to model the relationship between two or more explanatory variables and a response variable by fitting a linear equation to observed data.

In this context, we propose nonlinear models to predict the machining force components; the mathematical formulation is given by the following equations:

$$F_f = K_1 \cdot HRC^{\alpha_1} \cdot V_c^{\beta_1} \cdot f^{\gamma_1} \cdot a_p^{\delta_1}, \quad (4)$$

$$F_r = K_2 \cdot HRC^{\alpha_2} \cdot V_c^{\beta_2} \cdot f^{\gamma_2} \cdot a_p^{\delta_2}. \quad (5)$$

$$F_t = K_3 \cdot HRC^{\alpha_3} \cdot V_c^{\beta_3} \cdot f^{\gamma_3} \cdot a_p^{\delta_3}. \quad (6)$$

These equations are put in linear form by using the natural logarithm as follows:

$$\ln(F_f) = \ln K_1 + \alpha_1 \ln HRC + \beta_1 \ln V_c + \gamma_1 \ln f + \delta_1 \ln a_p. \quad (7)$$

$$\ln(F_r) = \ln K_2 + \alpha_2 \ln HRC + \beta_2 \ln V_c + \gamma_2 \ln f + \delta_2 \ln a_p. \quad (8)$$

$$\ln(F_t) = \ln K_3 + \alpha_3 \ln HRC + \beta_3 \ln V_c + \gamma_3 \ln f + \delta_3 \ln a_p. \quad (9)$$

The variables to be explained by the MLR models are: $\ln(F_f)$, $\ln(F_r)$ and $\ln(F_t)$, and the independent variables are: $\ln(HRC)$, $\ln(V_c)$, $\ln(f)$ and $\ln(a_p)$.

2.1. Experimental dataset for training and testing the developed ANN

The main objective of the experimental work was to investigate the influence of cutting parameters (V_c , f and a_p) and workpiece hardness (HRC) on machining force in hard turning of AISI 52100 bearing steel using CBN cutting tool. The components of machining force were measured by a piezoelectric dynamometer Kistler type 9257B.

The AISI 52100 bearing steel with the following chemical composition was used as workpiece in turning: 1.05% C; 1.481% Cr; 0.033% Cu; 0.018% S; 0.239% Si; 0.01% Mo; 0.365% Mn; 0.009% P. After heat treatment an average hardness from 45 to 55.25 HRC was obtained. CBN inserts VBGW160408NC-2 (Sumitomo) were used to machining AISI 52100 bearing steel under CNC lathe type Ramo (RACN82).

The experimental dataset is divided into two databases as training and test bases. On a total of 35 examples, 70% will be intended for the training and 30% will be reserved for the test. The training of the developed ANN is performed on 25 pairs of input-target dataset as shown on Table 1.

The generalization capability is evaluated on 10 further pairs of input-target dataset (Table 2) that were not been used in training dataset.

Notice that before training and testing the network, the values which are set of input and target vectors are normalized in the range of -1 to 1 for efficient processing by the ANN.

Training dataset [10]

Test n^o	Machining parameters				Experimental components of cutting force		
	HRC	V_c , m/min	f , mm/rev	a_p , mm	F_f , N	F_r , N	F_t , N
1	45	100	0.1	0.2	55.81	102.60	127.14
2	45	150	0.05	0.2	20.23	50.52	50.04
3	45	150	0.1	0.2	27.64	70.66	82.64
4	45	150	0.1	0.3	60.05	117.77	135.27
5	45	150	0.15	0.2	42.25	115.01	135.60
6	45	200	0.1	0.2	32.82	78.86	90.70
7	50	100	0.1	0.2	41.36	110.99	106.12
8	50	150	0.05	0.2	34.89	102.99	68.77
9	50	150	0.1	0.4	90.41	157.68	178.67
10	50	150	0.2	0.2	58.09	193.25	168.47
11	50	200	0.1	0.1	35.84	97.29	93.98
12	51.5	50	0.1	0.2	44.31	102.87	116.84
13	51.5	150	0.1	0.2	37.73	101.78	97.76
14	51.5	250	0.1	0.2	36.80	96.79	94.55
15	51.5	300	0.1	0.4	59.04	111.98	135.02
16	54	100	0.1	0.2	34.01	85.25	96.05
17	54	150	0.05	0.2	23.40	58.13	55.61
18	54	150	0.1	0.3	57.34	114.92	131.04
19	54	150	0.15	0.2	40.27	110.19	127.85
20	54	150	0.2	0.2	45.01	140.02	159.01
21	54	200	0.1	0.2	35.26	91.26	92.00
22	55.25	50	0.1	0.2	51.46	140.99	120.74
23	55.25	150	0.1	0.2	29.57	74.71	86.18
24	55.25	200	0.1	0.2	17.90	57.63	61.39
25	55.25	300	0.1	0.2	32.36	97.29	91.68

Table 2

Testing dataset [10]

Test n^o	Machining parameters				Experimental components of cutting force		
	HRC	V_c , m/min	f , mm/rev	a_p , mm	F_f , N	F_r , N	F_t , N
26	45	150	0.08	0.2	28.01	68.62	75.25
27	45	150	0.12	0.1	16.04	60.37	62.84
28	50	150	0.1	0.3	65.80	154.11	142.81
29	50	150	0.15	0.2	46.37	139.42	136.84
30	51.5	50	0.1	0.4	57.83	115.47	140.18
31	51.5	300	0.1	0.2	32.29	89.28	92.64
32	54	150	0.1	0.2	32.30	90.61	93.54
33	54	150	0.1	0.4	82.76	142.35	172.37
34	55.25	100	0.1	0.2	33.38	80.99	95.66
35	55.25	250	0.1	0.2	33.48	77.61	92.81

2.2. Optimal network architecture and simulation results

The best results for training are obtained when the transfer function of the output layer is linear and it is hyperbolic tangent sigmoid for the hidden layer.

In the same context, Table 3 shows a comparative study between two configurations during training. For the first configuration (S/L), the transfer function of the output layer is linear and it is hyperbolic tangent sigmoid for the hidden layer. On the other hand, for the second configuration (S/S), the transfer functions of the output and hidden layers are hyperbolic tangent sigmoid.

The representative criteria, adopted for (S/L) and (S/S) configurations, is the linear regression coefficient R .

From Table 3, we can see that the (S/L) configuration gives the best coefficient R during training phase.

In order to define the optimal architecture, a various number of neurons in the hidden layer have been tested from 1 to 12 with step of 1. Four representative criteria are adopted for each structure and collected in Table 4; namely: SSE, SSW, R for training and testing, and MAPE Testing.

Comparison between (S/L) and (S/S) configurations

ANN Structure	<i>R</i> - Training (S/L)	<i>R</i> - Training (S/S)
4-1-3	0.878	0.562
4-2-3	0.921	-0.131
4-3-3	0.962	0.351
4-4-3	0.982	0.216
4-5-3	0.985	-0.131
4-6-3	0.997	0.647
4-7-3	0.999	0.703
4-8-3	0.999	0.620
4-9-3	0.999	0.113
4-10-3	0.999	0.818
4-11-3	1	0.485
4-12-3	1	0.518

Table 4

Criteria values for each structure

ANN Structure	SSE	SSW	<i>R</i> - Training	<i>R</i> - Testing	MAPE Testing (%)
4-1-3	15.771	0.121	0.199	0.207	35.76
4-2-3	2.465	33.158	0.921	0.841	18.32
4-3-3	2.214	38.213	0.930	0.828	18.26
4-4-3	0.705	102.809	0.978	0.866	19.31
4-5-3	2.063	40.340	0.935	0.826	18.71
4-6-3	2.035	41.149	0.936	0.823	18.92
4-7-3	0.082	192.444	0.997	0.910	14.28
4-8-3	0.043	212.589	0.998	0.922	14.24
4-9-3	0.007	246.724	0.999	0.845	18.56
4-10-3	2.056	40.395	0.935	0.825	18.72
4-11-3	0.004	223.386	0.999	0.934	13.00
4-12-3	2.039	40.946	0.935	0.824	18.85

From Table 4, we can see that the structure consisting of 11 neurons in hidden layer is chosen as the optimum ANN structure. Notice that the training algorithm converges if the SSE and the SSW are relatively constant over several iterations for each structure; the error of the network is minimized and then the best network architecture is selected.

The evolution of SSE value as a function of SSW value is plotted on Fig. 4.

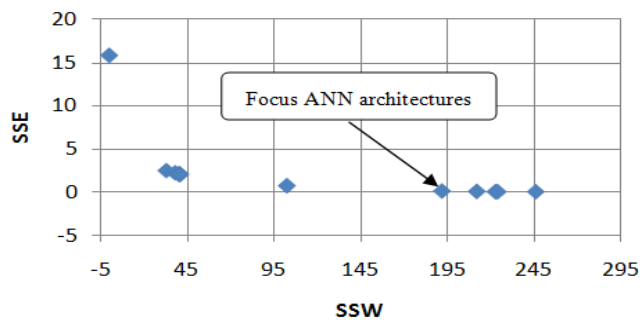


Fig. 4 Decrease of SSE during training of different ANN structures

Notice that the best ANN structure is chosen in the convergence area where SSE is slightly close to 0 and SSW is between 192 and 247. For this area, it can be seen from Table 4 that the number of neurons in hidden layer must reach 7.

Let us recall, that the developed ANN consists of

4 inputs and of an output layer having 3 neurons. Also, the results given in Tables 3 and 4 are obtained for a single hidden layer. To show the influence of the number of hidden layers, two structures were adopted; in the first one, the single hidden layer has 11 neurons, and the second structure makes up of two hidden layers having respectively 6 and 11 neurons. Fig. 5 illustrates a graphical comparison between the two structures for the prediction of tangential force during training.

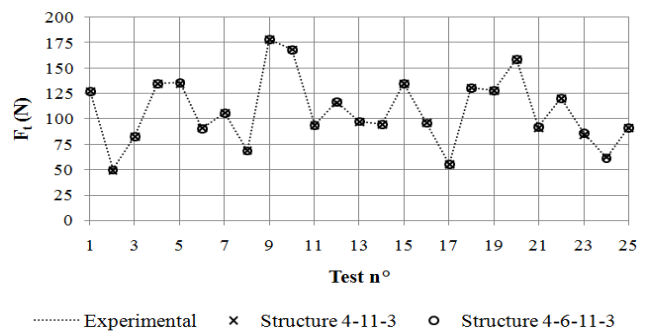


Fig. 5 Comparison between 4-11-3 and 4-6-11-3 structures

According to the last figure, it is preferable to choose only one hidden layer because the two structures give the same results.

Under Matlab Neural Network Toolbox, the developed ANN can be shown as follows in Fig. 6.

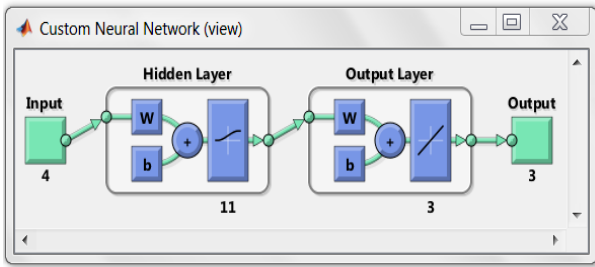


Fig. 6 Developed ANN structure under Matlab

The optimal architecture of the developed ANN consists of multilayer feed-forward with 4-11-3 structure. Back-Propagation (BP) by Bayesian Regularization (BR) in combination with Levenberg–Marquardt (LM) algorithm is employed for training.

Table 5 gives a numerical comparison between experimental and predicted machining force components during training phase.

Table 5

Comparison between experimental and predicted values of machining force components during training

Test n°	Experimental components			Predicted components			MAPE (%)		
	F_f	F_r	F_t	F_f	F_r	F_t	(F_f)	(F_r)	(F_t)
1	55.81	102.60	127.14	55.31	103.08	127.73	0.89	0.47	0.46
2	20.23	50.52	50.04	20.52	50.79	49.38	1.47	0.53	1.32
3	27.64	70.66	82.64	27.85	69.89	82.99	0.77	1.09	0.41
4	60.05	117.77	135.27	60.21	117.63	135.00	0.27	0.12	0.20
5	42.25	115.01	135.60	42.57	114.99	134.92	0.75	0.02	0.50
6	32.82	78.86	90.70	32.37	79.09	91.24	1.37	0.29	0.60
7	41.36	110.99	106.12	41.37	110.40	106.29	0.02	0.54	0.16
8	34.89	102.99	68.77	34.65	102.81	69.12	0.69	0.17	0.51
9	90.41	157.68	178.67	90.32	157.80	178.72	0.10	0.08	0.03
10	58.09	193.25	168.47	57.96	193.26	168.76	0.23	0.00	0.17
11	35.84	97.29	93.98	35.87	97.23	93.86	0.09	0.06	0.13
12	44.31	102.87	116.84	44.53	102.78	116.52	0.49	0.09	0.28
13	37.73	101.78	97.76	38.01	103.04	97.28	0.74	1.24	0.49
14	36.80	96.79	94.55	37.00	96.76	94.48	0.55	0.03	0.08
15	59.04	111.98	135.02	59.05	111.97	135.02	0.00	0.00	0.00
16	34.01	85.25	96.05	33.50	85.79	96.72	1.52	0.64	0.70
17	23.40	58.13	55.61	23.32	58.25	55.71	0.36	0.20	0.18
18	57.34	114.92	131.04	57.38	114.77	131.08	0.07	0.13	0.04
19	40.27	110.19	127.85	39.95	110.27	128.33	0.78	0.07	0.38
Test n°	Experimental components			Predicted components			MAPE (%)		
	F_f	F_r	F_t	F_f	F_r	F_t	(F_f)	(F_r)	(F_t)
20	45.01	140.02	159.01	45.15	140.01	158.72	0.31	0.00	0.18
21	35.26	91.26	92.00	35.22	89.79	91.41	0.12	1.62	0.65
22	51.46	140.99	120.74	51.59	140.74	120.65	0.26	0.18	0.07
23	29.57	74.71	86.18	30.09	74.44	84.88	1.75	0.36	1.50
24	17.90	57.63	61.39	17.72	58.34	62.80	1.02	1.24	2.30
25	32.36	97.29	91.68	32.34	97.48	91.52	0.04	0.20	0.17
Average MAPE (%)							0.59	0.37	0.46

The developed ANN gives precise results for the prediction of machining force components during training phase; average MAPEs of 0.59 %, 0.37 % and 0.46 % are respectively noted on F_f , F_r and F_t .

Table 6 illustrates cutting conditions used to test the developed ANN as well as the corresponding experimental and predicted machining force components.

Table 6

Comparison between experimental and predicted values during test

Test n°	Experimental components			Predicted components			MAPE (%)		
	F_f	F_r	F_t	F_f	F_r	F_t	(F_f)	(F_r)	(F_t)
26	55.81	102.60	127.14	55.31	103.08	127.73	0.89	0.47	0.46
27	20.23	50.52	50.04	20.52	50.79	49.38	1.47	0.53	1.32
28	27.64	70.66	82.64	27.85	69.89	82.99	0.77	1.09	0.41
29	60.05	117.77	135.27	60.21	117.63	135.00	0.27	0.12	0.20

Comparison between experimental and predicted values during test

Test n	Experimental components			Predicted components			MAPE (%)		
30	42.25	115.01	135.60	42.57	114.99	134.92	0.75	0.02	0.50
31	32.82	78.86	90.70	32.37	79.09	91.24	1.37	0.29	0.60
32	41.36	110.99	106.12	41.37	110.40	106.29	0.02	0.54	0.16
33	34.89	102.99	68.77	34.65	102.81	69.12	0.69	0.17	0.51
34	90.41	157.68	178.67	90.32	157.80	178.72	0.10	0.08	0.03
35	58.09	193.25	168.47	57.96	193.26	168.76	0.23	0.00	0.17
Average MAPE (%)							14.55	12.73	11.73

The average MAPEs of 14.55%, 12.73% and 11.73% are respectively noted on F_f , F_r and F_t during the test phase.

Fig. 7 illustrates a graphical comparison between experimental and predicted machining force components for test phase.

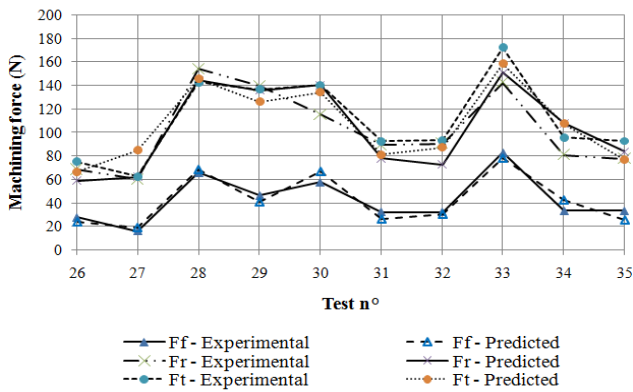


Fig. 7 Comparison between experimental and predicted machining force components during test phase

Tables 7 and 8 gives respectively the performances of the developed ANN and the analysis of variance as follows.

Table 7

Performances of the developed ANN

Structure	SSE	SSW	R - Training	R - Testing	R - ANN
4-11-3	0.004	223.386	0.999	0.934	0.978
Linear regression coefficients					
$R^2 (F_f) = 96.7 \%$		$R^2 (F_r) = 94.5 \%$		$R^2 (F_t) = 96.1 \%$	
Average MAPEs for the ANN					
4.58 % for (F_f)		3.90 % for (F_r)		3.68 % for (F_t)	

Table 8

Analysis of variance for the ANN approach

Source		Sum of Squares	Df	Mean Square	F-Ratio
F_f	Model	10001.80	4	2500.45	220.34
	Residual	340.45	30	11.35	
F_r	Model	36439.01	4	9109.75	128.99
	Residual	2118.70	30	70.62	
F_t	Model	36703.57	4	9175.89	184.83
	Residual	1489.37	30	49.65	

2.3. Multiple Linear Regression modeling

The prediction models of the machining force components with MLR are given by the following equations:

- the component F_f with $R^2 = 92.5 \%$ is expressed by:

$$\ln(F_f) = 7.31419 + 0.17844 \cdot \ln HRC - 0.21268 \cdot \ln V_c + 0.60292 \cdot \ln f + 1.25507 \cdot \ln a_p \quad (10)$$

- the component F_r with $R^2 = 82.2 \%$ is voiced by:

$$\ln(F_r) = 7.11439 + 0.29941 \cdot \ln HRC - 0.17022 \cdot \ln V_c + 0.78193 \cdot \ln f + 0.70274 \cdot \ln a_p \quad (11)$$

- the component F_t with $R^2 = 96.6 \%$ is given by:

$$\ln(F_t) = 8.02677 + 0.12830 \cdot \ln HRC - 0.15214 \cdot \ln V_c + 0.82226 \cdot \ln f + 0.81963 \cdot \ln a_p \quad (12)$$

From these equations, we can see that the machining force components increase with the augmentation of workpiece hardness, feed and depth-of-cut; but, it decreases with the augmentation of cutting speed.

Table 9 gives the analysis of variance for Multiple Linear Regression modeling. Notice that the tests n° 1, 8, 11, 24 and 30 are eliminated to avoid studentized residuals greater than 3 in absolute value and to give best performances (high linear regression coefficient R).

Table 9

Analysis of variance for MLR modeling

Source		Sum of Squares	Df	Mean Square	F-Ratio
$\ln F_f$	Model	4.03937	4	1.00984	77.05
	Residual	0.327677	25	0.013107	
$\ln F_r$	Model	2.44779	4	0.61195	28.82
	Residual	0.530796	25	0.021232	
$\ln F_t$	Model	2.85884	4	0.71471	179.48
	Residual	0.099553	25	0.003982	

Table 10 gives the analysis of variance by considering all tests (35 examples) as follows.

Notice that the squared linear regression coefficients of 75.9%, 67.6% and 84.7% are respectively noted

on (F_f) , (F_r) and (F_t) by considering all tests (35 examples).

Table 11 gives a numerical comparison between experimental and predicted MLR values of the machining force components.

It can be seen that the MLR modeling gives the average MAPEs of 16.15%, 15.71% and 9.37% which are respectively noted on F_f , F_r and F_t .

Table 10
Analysis of variance for MLR modeling (all tests)

Source		Sum of Squares	Df	Mean Square	F-Ratio
F_f	Model	12851.95	4	3212.99	23.66
	Residual	4073.71	30	135.79	
F_r	Model	34696.88	4	8674.22	15.64
	Residual	16639.82	30	554.66	
F_t	Model	46959.94	4	11739.98	41.63
	Residual	8460.69	30	282.02	

Table 11
Comparison between experimental and predicted MLR values of the machining force components

Test n°	Experimental components			Predicted components			MAPE (%)		
	F_f	F_r	F_t	F_f	F_r	F_t	(F_f)	(F_r)	(F_t)
1	55.81	102.60	127.14	36.81	93.58	99.69	34.04	8.80	21.59
2	20.23	50.52	50.04	22.23	50.79	53.01	9.91	0.54	5.93
3	27.64	70.66	82.64	33.77	87.34	93.73	22.18	23.60	13.42
4	60.05	117.77	135.27	56.17	116.13	130.68	6.46	1.39	3.39
5	42.25	115.01	135.60	43.12	119.92	130.82	2.06	4.27	3.53
6	32.82	78.86	90.70	31.77	83.16	89.72	3.21	5.46	1.08
7	41.36	110.99	106.12	37.51	96.58	101.05	9.31	12.99	4.78
8	34.89	102.99	68.77	22.66	52.42	53.73	35.06	49.10	21.87
9	90.41	157.68	178.67	82.13	146.70	167.68	9.16	6.96	6.15
10	58.09	193.25	168.47	52.26	154.98	167.99	10.03	19.80	0.29
11	35.84	97.29	93.98	13.56	52.73	51.52	62.16	45.80	45.18
12	44.31	102.87	116.84	43.70	109.64	112.72	1.38	6.58	3.53
Test n°	Experimental components			Predicted components			MAPE (%)		
	F_f	F_r	F_t	F_f	F_r	F_t	(F_f)	(F_r)	(F_t)
13	37.73	101.78	97.76	34.59	90.94	95.37	8.32	10.65	2.45
14	36.80	96.79	94.55	31.03	83.36	88.24	15.68	13.87	6.68
15	59.04	111.98	135.02	71.25	131.53	151.47	20.68	17.46	12.18
16	34.01	85.25	96.05	38.03	98.83	102.05	11.81	15.93	6.25
17	23.40	58.13	55.61	22.97	53.64	54.26	1.84	7.72	2.42
18	57.34	114.92	131.04	58.03	122.64	133.77	1.21	6.72	2.09
19	40.27	110.19	127.85	44.55	126.65	133.92	10.62	14.93	4.74
20	45.01	140.02	159.01	52.98	158.59	169.65	17.72	13.26	6.69
21	35.26	91.26	92.00	32.82	87.83	91.84	6.93	3.76	0.17
22	51.46	140.99	120.74	44.25	111.97	113.74	14.01	20.59	5.80
23	29.57	74.71	86.18	35.03	92.87	96.23	18.46	24.31	11.66
24	17.90	57.63	61.39	32.95	88.43	92.11	84.08	53.45	50.04
25	32.36	97.29	91.68	30.23	82.53	86.60	6.59	15.17	5.54
26	28.01	68.62	75.25	29.52	73.35	78.02	5.39	6.90	3.68
27	16.04	60.37	62.84	15.79	61.88	61.70	1.54	2.50	1.82
28	65.80	154.11	142.81	57.24	119.85	132.46	13.01	22.23	7.25
29	46.37	139.42	136.84	43.94	123.76	132.60	5.24	11.23	3.10
30	57.83	115.47	140.18	104.30	178.44	198.94	80.35	54.53	41.92
31	32.29	89.28	92.64	29.85	80.82	85.82	7.55	9.48	7.36
32	32.30	90.61	93.54	34.89	92.24	95.95	8.01	1.79	2.57
33	82.76	142.35	172.37	83.27	150.12	169.34	0.61	5.46	1.76
34	33.38	80.99	95.66	38.18	99.51	102.35	14.39	22.86	7.00
35	33.48	77.61	92.81	31.42	85.14	89.04	6.14	9.70	4.07
Average MAPE (%)							16.15	15.71	9.37

3. Comparison between ANN and MLR predictions

For comparison between the values of the machining force components predicted by ANN and MLR modeling, the Root Mean Square Error (RMSE) [7] was used:

$$RMSE = \sqrt{\frac{\sum_{k=1}^Q (c(k) - s(k))^2}{Q}} \quad (13)$$

The Table 12 gives the RMSEs obtained by ANN and MLR modeling.

The results revealed that the ANN approach resulted into minimum RMSEs of the predicted machining force components compared to those obtained by MLR modeling. Also, the ANN approach gives minimum MAPEs, minimum mean square of residual sources and high squared linear regression coefficients. Notice, that the F-Ratios for ANN approach are greater than obtained by

MLR modeling; for this purpose, the ANN regression is globally very significant.

Table 12

Comparison between RMSEs obtained by ANN and MLR modeling

Test no.	Predicted values by ANN			Predicted values by MLR		
	F_f	F_r	F_t	F_f	F_r	F_t
1	55.31	103.08	127.73	36.81	93.58	99.69
2	20.52	50.79	49.38	22.23	50.79	53.01
Test no.	Predicted values by ANN			Predicted values by MLR		
	F_f	F_r	F_t	F_f	F_r	F_t
3	27.85	69.89	82.99	33.77	87.34	93.73
4	60.21	117.63	135.00	56.17	116.13	130.68
5	42.57	114.99	134.92	43.12	119.92	130.82
6	32.37	79.09	91.24	31.77	83.16	89.72
7	41.37	110.40	106.29	37.51	96.58	101.05
8	34.65	102.81	69.12	22.66	52.42	53.73
9	90.32	157.80	178.72	82.13	146.70	167.68
10	57.96	193.26	168.76	52.26	154.98	167.99
11	35.87	97.23	93.86	13.56	52.73	51.52
12	44.53	102.78	116.52	43.70	109.64	112.72
13	38.01	103.04	97.28	34.59	90.94	95.37
14	37.00	96.76	94.48	31.03	83.36	88.24
15	59.05	111.97	135.02	71.25	131.53	151.47
16	33.50	85.79	96.72	38.03	98.83	102.05
17	23.32	58.25	55.71	22.97	53.64	54.26
18	57.38	114.77	131.08	58.03	122.64	133.77
19	39.95	110.27	128.33	44.55	126.65	133.92
20	45.15	140.01	158.72	52.98	158.59	169.65
21	35.22	89.79	91.41	32.82	87.83	91.84
22	51.59	140.74	120.65	44.25	111.97	113.74
Test no.	Predicted values by ANN			Predicted values by MLR		
	F_f	F_r	F_t	F_f	F_r	F_t
23	30.09	74.44	84.88	35.03	92.87	96.23
24	17.72	58.34	62.80	32.95	88.43	92.11
25	32.34	97.48	91.52	30.23	82.53	86.60
26	24.05	59.12	66.76	29.52	73.35	78.02
27	19.48	62.40	85.10	15.79	61.88	61.70
28	68.51	144.38	145.46	57.24	119.85	132.46
29	41.20	136.10	126.03	43.94	123.76	132.60
30	66.69	140.55	134.11	104.30	178.44	198.94
31	26.54	77.99	81.46	29.85	80.82	85.82
32	30.40	72.76	87.30	34.89	92.24	95.95
33	78.12	151.01	158.59	83.27	150.12	169.34
34	42.42	107.90	107.46	38.18	99.51	102.35
35	25.81	83.84	76.67	31.42	85.14	89.04
RMSE	3.12	7.78	6.52	10.79	21.80	15.55

4. Conclusions

The objective of this study is to develop an optimal ANN for prediction of machining force components in hard turning of AISI 52100 bearing steel with CBN cutting tool.

ANN training is performed on an experimental machining dataset of 25 examples and then the numerical model accuracy is evaluated on a further dataset of 10 values not used in training. Back-propagation training is performed by using Bayesian Regularization in combination with Levenberg-Marquardt algorithm. Hyperbolic tangent sigmoid transfer function is chosen in hidden layer

and a linear one in output layer. Four criteria are used to evaluate the ANN efficiency: SSE, SSW, linear regression coefficient R and MAPE between ANN prediction and experimental values. A various number of neurons in hidden layer are tested; it is noticed that the optimal architecture is obtained when this number reaches 11.

To show the effectiveness of the developed ANN, the results of machining force prediction are confronted with experimental data and to those obtained by MLR modeling. A good agreement is found between experimental and predicted values of the machining force components. The results revealed that the ANN approach resulted into minimum RMSEs of the predicted machining force components compared to those obtained by MLR modeling. Also, the ANN approach gives minimum MAPEs, minimum mean square of residual sources and high squared linear regression coefficients. Finally, the regression by ANN approach is globally very significant.

References

1. **Luong, L. H. S.; Spedding, T. A.** 1995. A neural network system for predicting machining behavior, *Journal of Materials Processing Technology* 52: 585–591. [http://dx.doi.org/10.1016/0924-0136\(94\)01626-C](http://dx.doi.org/10.1016/0924-0136(94)01626-C).
2. **Szecs, T.** 1999. Cutting force modeling using artificial neural networks, *Journal of Materials Processing Technology* (92-93): 344- 349. [http://dx.doi.org/10.1016/S0924-0136\(99\)00183-1](http://dx.doi.org/10.1016/S0924-0136(99)00183-1).
3. **Ezugwu, E. O.; Fadare, D. A.; Bonney, J.; Da Silva, R. B.; Sales, W. F.** 2005. Modeling the correlation between cutting and process parameters in high-speed machining of Inconel 718 alloy using an artificial neural network, *International Journal of Machine Tools and Manufacture* (45): 1375–1385. <http://dx.doi.org/10.1016/j.ijmachtools.2005.02.004>.
4. **Hao, W.; Zhu, X.; Li, X.; Turyagyenda, G.** 2006. Prediction of cutting force for self-propelled rotary tool using artificial neural networks, *Journal of Materials Processing Technology*. (180): 23–29. <http://dx.doi.org/10.1016/j.jmatprotec.2006.04.123>
5. **Sharma, V. S.; Dhiman, S.; Sehgal, R.; Sharma, S. K.** 2008. Estimation of cutting forces and surface roughness for hard turning using neural networks, *Journal of Intelligent Manufacturing* 19 (4): 473–483. <http://dx.doi.org/10.1007/s10845-008-0097-1>.
6. **Özel, T.; Esteves Correia, A.; Paulo Davim, J.** 2009. Neural network process modeling for turning of steel parts using conventional and wiper inserts, *International Journal of Materials and Product Technology* 35 (Nos. ½): 246-258. <http://dx.doi.org/10.1504/IJMPT.2009.025230>.
7. **Madić, M.; Radovavić, M.** 2011. Methodology of developing optimal BP-ANN model for the prediction of cutting force in turning using Early Stopping method, *Facta Universitatis, Series: Mechanical Engineering* 9 (1): 21-32. UDC 007.52, 621.941, 519.863.
8. **Upadhyay, V.; Jain, P. K.; Mehta, N. K.** 2011. Artificial Neural Network Modeling of Cutting Force in Turning of Ti-6Al-4V Alloy and Its Comparison with Response Surface Methodology, *Proceedings of the International Conference on Soft Computing for Problem*

- Solving (SocProS) December 20-22, *Advances in Intelligent and Soft Computing* (131): 761-768.
<http://dx.doi.org/10.1007/978-81-322-0491-6>.
9. **Cica, D.; Sredanovic, B; Lakic-Globocki, G.; Kramar D.** 2013. Modeling of the cutting forces in turning process using various methods of cooling and lubricating: An artificial intelligence approach advances in mechanical engineering, Article ID 798597: 8 pages.
<http://dx.doi.org/10.1155/2013/798597>.
 10. **Makhfi, S.; Velasco, R.; Habak, M.; Haddouche, K.; Vantomme, P.** 2013. An Optimized ANN Approach for Cutting Forces Prediction in AISI 52100 Bearing Steel Hard Turning, *Science and Technology* 3(1): 24-32.
<http://dx.doi.org/10.5923/j.scit.20130301.03>.
 11. **Kara, F.; Aslantas, K.; Çiçek, A.** 2015. ANN and multiple regression method-based modeling of cutting forces in orthogonal machining of AISI 316L stainless steel, *Neural Computing and Applications* 26 (1): 237–250.
<http://dx.doi.org/10.1007/S00521-014-1721-y>.
 12. **Sharma, R. K.; Maurya, S.; Ranganath, M. S.; Vipin,** 2016. Artificial Neural Network Modeling for Surface Roughness and Cutting Force during Conventional Turning Process, *International Journal of Advanced Production and Industrial Engineering* 1(3): 01-05.
 IJAPIE-2016-07-301, VOL 1(3), 01-05.
 13. **Hagan, M. T.; Demuth, H. B.; Beale M. H.; De Jesús, O.** 2014. *Neural Network Design*. 2nd Edition eBook.
 ISBN 978-0-9717321-1-7
 14. **Montgomery D. C.** 2005. *Design and Analysis of Experiments*. 6th Edition.
 ISBN 0-471-48735-X

S. Makhfi, K. Haddouche, A. Bourdim, M. Habak

MODELING OF MACHINING FORCE IN HARD TURNING PROCESS

S u m m a r y

In this work, we develop a modeling based on an Artificial Neural Network (ANN) and Multiple Linear Regression (MLR) to predict the machining force components generated during hard turning of a bearing steel with CBN cutting tool. The inputs of the ANN model were the cutting parameters (cutting speed, feed and depth-of-cut) and the workpiece hardness. The network training is performed by using experimental data. The optimal network architecture is determined after several simulations by Matlab Neural Network Toolbox. Back-propagation by Bayesian Regularization in combination with Levenberg–Marquardt algorithm is employed for training. The ANN approach is suitable to estimate the machining force components such as feed-force, radial-force and tangential-force; for this purpose, the results are compared to those obtained by experiment, and the maximum average MAPE value of 4.58% was obtained for the machining force prediction. Also, the ANN results were compared to those obtained by MLR model. It was shown that the ANN model produced more successful results.

Keywords: modeling, machining force, hard turning, bearing steel, CBN cutting tool, Artificial Neural Network, Multiple Linear Regression.

Received October 03, 2017

Accepted June 14, 2018